ELSEVIER

International Journal of Mass Spectrometry 202 (2000) 299–313

International Journal of Mass Spectrometry

Reactions of angiotensin ions with hydroiodic acid

T. Gregory Schaaff, James L. Stephenson Jr., Scott A. McLuckey*

Chemical and Analytical Sciences Division, Oak Ridge National Laboratory, Oak Ridge, TN 37831-6365, USA

Received 23 May 2000; accepted 23 May 2000

Abstract

The kinetics of HI attachment to gaseous angiotensin-related ions were determined in a quadrupole ion trap mass spectrometer. The $(M + H)^+$ and $(M + 2H)^{2+}$ ions of peptides with sequences of DRVYIHPFHL, NRVYVHPFHL, and RVYIHPFHL and the $(M + H)^+$ ions of DRVYIHPF and NRVYVHPF and their respective methyl esters were studied. For many of the ions studied here, multiple reactive conformations were resolved by their differing reactivities. The kinetics of the attachment of HI to the singly charged ions are consistent with structural models that are generated by molecular mechanics calculations, which suggest a high degree of intraionic interactions between the protonation site and other basic sites in the ion. The incorporation of HI can also disrupt the inherent intraionic interactions in the ions, which is not only reflected in the reaction kinetics, but also consistent with the interactions suggested by the molecular mechanics simulations. These results confirm that HI attachment kinetics can be used as a probe of three dimensional ion structure and provide important new information regarding the utility of this molecular probe. (Int J Mass Spectrom 202 (2000) 299–313) © 2000 Elsevier Science B.V.

Keywords: Angiotensin ions; Hydroiodic acid attachment; Quadrupole ion trap

1. Introduction

Gas phase ions that are derived from polypeptides constitute a fundamentally interesting and increasingly important class of ions that can be studied by a variety of mass spectrometric techniques. One of the most common mass spectrometric studies of polypeptides is the unimolecular dissociation of these ions [1,2], which is typically induced by energetic collisions with either target gases [3–5] or surfaces [6,7]. The dissociation products generated by these methods can be used to identify peptides from enzymatic digestions and consequently, their parent proteins. The influence of the primary structure on the dissociation properties of peptides has been implicated in many studies. However, from an increasing number of reports, the overall ion structure (i.e. three-dimensional gas phase structure) may well be one of the more important factors influencing the dissociation of polypeptide ions [8–15]. Thus, methods to provide three-dimensional structural information regarding gas phase peptide ions are being pursued.

The inherent ion conformation and reactivity of large ionized polypeptides is linked to the intraionic interactions that can occur within the ion in the gas phase. The three-dimensional structures that ions can adopt in the gas-phase can be probed by methods that measure the ion's collision cross section [16–20] or

* Corresponding author. Current address: 1393 Brown Laboratory, Department of Chemistry, Purdue University, West Lafayette, IN 47907-1393. E-mail: mcluckey@purdue.edu

PII S1387-3806(00)00255-4

its chemical reactivity [21]. Ion mobility measurements have shown that the overall shape of protein ions can be influenced by the charge state, degree of solvation and the temperature of the ions [22–24]. In some cases, multiple conformations can exist for ions with the same nominal *m/z* values [19,25–27].

Many reagent molecules have been suggested for their utility in probing ion structures as they relate to the ion reactivity. The resulting ion/molecule reactions have primarily been associated with mechanisms that directly probe the charge site of the ion (e.g. H/D exchange [9,28,29] and proton transfer [30–36]). Both D_2O H/D exchange and proton transfer gas phase reactions have illustrated that these ion/molecule reactions can detect the presence of different reactive conformations, and lay the basis for qualitative hypotheses concerning the gas phase ion structure [31–33,35–39]. However, ion/molecule reactions using HI as the molecular probe proceed through a quite different (and complementary) mechanism: attachment of HI to a neutral (nonprotonated) basic site (e.g. free N-terminus, histidine, lysine, arginine) [40,41]. Likewise, the kinetics of the HI attachment reactions and H/D exchange using DI have been shown to detect the presence of multiple reactive conformations of protein and peptide ions [42–44].

Angiotensin I, angiotensin II and their structural analogs represent a set of peptide ions that lend themselves well to ion/molecule reactions and other mass spectral studies concerning intraionic interactions. Although these peptides are relatively small, they are still quite complex, with multiple acidic and basic groups present in their amino acid sequences. Thus, it is expected that extensive intraionic interactions exist, which can be probed by both physical and chemical methods. Here, we present the HI addition kinetic data for various ions of angiotensin I, angiotensin II and their structural analogs. These studies demonstrate that multiple ion conformations can be detected using HI as a gas phase molecular probe. Aspects of the observed reaction kinetics are consistent with the intraionic interactions that are predicted by molecular mechanics calculations. In addition, the HI attachment kinetics for this small polypeptide also reveal that the attachment of HI to an ion may disrupt the intraionic interactions, thereby changing the ion's reactivity and structure during the reaction.

2. Experimental

Angiotensin-I (DRVYIHPFHL), angiotensin-II (DRVYIHPF), and goosefish angiotensin (NRVYVHPFHL) were purchased from Sigma Chemicals (St. Louis, MO). Goosefish angiotensin II (NRVYVHPF) was purchased from Research Genetics (Huntsville, AL). All peptides were used without any further purification. The O-methyl ester of each peptide was synthesized at 50–100 nmol quantities, as previously described [45,46]. The reagents used were HPLC grade or better and deionized water was purified to 18 $\mu\Omega$ with a Millipore (Bedford, MA) water purification system. The concentration of solutions used for electrospray infusion were between 10 and 20 pmol/μL in 100% methanol with 1% acetic acid. As previously found for bradykinin ions, the reaction kinetics were not affected by either concentration (10–50 pmol/μL) or by use of 100% water as the solvent composition.

A modified [47] Finnigan MAT ion trap mass spectrometer (San Jose, CA) was used to follow the angiotensin/HI reaction kinetics, which were measured as described in detail for bradykinin ions [42]. Due to the corrosive nature of the HI reactant, the ion trap analyzer main vacuum housing was evacuated by a Varian (Walnut Creek, CA) Turbo-V 550-ICE MacroTorr high corrosive applications turbomolecular pump, which was backed by a Varian SD-301 mechanical pump adapted with a caustic soda trap. The ion/molecule reactions were performed with a background pressure of 1 mTorr He in the ion trap maintained using a Granville-Phillips 203 (Boulder, CO) variable leak valve. The HI pressure was maintained and monitored throughout the experiments between 8×10^{-6} and 1.4×10^{-5} Torr (depending on the reactivity of the ion), and all pressures reported have been corrected for differences in ionization potentials of various gaseous species (HI, He) compared to the ion gauge calibration with N_2 [48]. The

base pressure of the instrument, i.e. before introduction of any gas, is $\sim 5 \times 10^{-7}$ Torr.

Pseudo-first-order kinetics prevail because the HI number density is constant and always much greater than the ion number density. Depending on the peptide and charge state, the gas phase reactions followed pseudo-first-order consecutive, parallel or parallel/consecutive kinetics. To determine the reaction rates, the rate of loss of reactant ion abundance (i.e. ion population generated by electrospray) was first plotted versus time and fit to a multidimensional exponential decay of the following form:

$$I(t) = \sum_{i=1}^{n} P_i(e^{-k_i t}) \quad (1)$$

where $I(t)$ is the ion abundance as a function of time, P is the ion population, k is the measured rate, and $n = 1, 2$, or 3. Consecutive and parallel/consecutive reactions were modeled and fit with a script generated and run using Microcal Origin 5.0 for WINDOWS, which allowed for the simultaneous fitting of all parameters [e.g. (1) all rates for consecutive reaction kinetics and (2) populations and respective rates for parallel/consecutive reaction kinetics]. The errors generated by the multidimensional fits were in the range from ~10% to 15% of the determined reaction parameter. In all cases, the rate(s) of loss of the initial ion population was used (as a constant value) in the fitting of the abundance profiles, since these values could be derived with highest confidence. The rate constants reported were calculated by dividing the determined reaction rate by the number density of HI.

Molecular mechanics calculations were performed in a manner similar to that outlined by many reports for modeling gas-phase structures of polypeptides [9,13,28,49,50]. All calculations were performed using the CVFF and CFF91 potentials provided with the FDISCOVER suite of programs and run on a Silicon Graphics O2 workstation with INSIGHTII interface software (Molecular Simulations Inc., CA). The structures of the angiotensin analogs were drawn using the INSIGHT 98 interface program. These structures were first minimized using a combination of steepest gradient, followed by conjugate gradient minimization routines. The minimized structures were (1) heated to 700 K over 300 ps, (2) annealed at 700 K for 1 ns, and (3) then cooled to 100 K over 300 ps. To prevent trans–cis conversions in the peptide backbone [51], the torsion restriction option provided by the software was used. The resulting structure (after cooling from 700 K) was quenched by minimizing the 100 K structure using steepest and conjugate gradient routines. The structure generated from the minimization/annealing/minimization strategy was annealed and minimized again. The structure of the ions generated by these steps were not dependent on the force field used for the calculation (CVFF versus CFF91). For all simulations, a step size of 1 fs was used. These steps were repeated until 10 consecutive structures were generated with total energies within 10% of the lowest energy structure found by this conformational search. Then, these 10 structures were used to generate 5 structures each for a total of 50 candidate structures for each ion of interest. For the singly charged ions, all ions were assumed to be protonated at the guanidinium group of the arginine residue.

3. Results

The rate constants for the addition of HI to the ions of angiotensin-type peptides were measured. Six of the peptides studied consisted of: (1) angiotensin-I (Ang-I), (2) goosefish angiotensin-I (GF-Ang-I), (3) des-Asp^1 angiotensin-I (des-Asp^1 Ang-I), and (4–6) the O-methyl ester of each. Four additional peptides were: (7) angiotensin-II (Ang-II), (8) goosefish angiotensin-II (GF-Ang-II), and (9 and 10) the O-methyl esters of these two peptides. The sequences of each of these peptides are shown in Scheme 1, where the basic sites are denoted by bold/italic lettering and the acidic sites are underlined.

The reactivity of angiotensin ions with HI in the gas phase is generally similar to the reactivity of other polypeptides that we have studied [40–42]. (1) The observed reaction behavior is consistent with the selective attachment of HI to available (nonprotonated) basic sites in the ion, e.g. arginine, lysine, histidine and the N-terminus. The kinetics of the

Angiotensin-I (Ang-I)
Asp–***Arg***–Val–Tyr–Ile–***His***–Pro–Phe–***His***–Leu

Goosefish Angiotensin-I (GF-Ang-I)
Asn–***Arg***–Val–Tyr–Val–***His***–Pro–Phe–***His***–Leu

des-Asp[1] Angiotensin-I (des-Asp-Ang-I)
Arg–Val–Tyr–Ile–***His***–Pro–Phe–***His***–Leu

Angiotensin-II (Ang-II)
Asp–***Arg***–Val–Tyr–Ile–***His***–Pro–Phe

Goosefish Angiotensin II (GF-Ang-II)
An–***Arg***–Val–Tyr–Val–***His***–Pro–Phe

Scheme 1.

reactions reflect the gas-phase basicity of the reactant site, as well as its geometric exposure to the attacking HI (i.e. steric factors). (2) The magnitude of the HI attachment rate constants is well below the ion/molecule collision rate and is in the same range as those previously found for other peptide ions. (3) Linear and nonlinear pseudofirst order reaction kinetics are measured for certain ions, indicating single and multiple ion conformations, respectively. (4) Derivatization of the peptide to form the O-methyl ester generally causes a decrease in the reaction rate constants for the addition of HI to the ion, but in some cases causes gross conformational changes, which are reflected in the reaction kinetics.

Thus, here we present data that is inherent to the angiotensin-type ions, which yields further information regarding the intraionic interactions that may be governing the kinetics of this gas phase reaction.

From studies with bradykinin and analog ions, the presence of acidic groups (e.g. carboxy terminus, aspartic acid and glutamic acid) can have a potentially dramatic effect on the reaction kinetics [42]. Thus, the amino acid sequences of the angiotensin analogs (Scheme 1) provide an interesting set of model systems to study the effects of multiple basic and acidic sites on the reactivity of peptide ions with gaseous hydroiodic acid (HI). For example, Ang-I contains four basic amino acid residues (i.e. N-terminus, one arginine, and two histidines, denoted in bold/italic) and two acidic sites (aspartic acid and the C-terminus, underlined). Thus, the $(M + nH)^{n+}$ ion should add $(4 - n)$ HI molecules. Ang-II, on the other hand, contains three basic sites (i.e. N-terminus, one arginine, and one histidine) so that the $(M + nH)^{n+}$ ion should add $(3 - n)$ HI molecules. However, for the species studied here (both Ang-I and Ang-II analogs), ions with only one possible attachment site were found to be nearly unreactive under our experimental conditions, i.e. reliable rate measurements could not be made over the storage time allowed for reactions. For example, the $(M + 3H)^{3+}$ ion of Ang-I, which should add 1 HI molecule is essentially unreactive, showing only a small extent of attachment with a reaction rate that is too small to measure reliably. To facilitate comparison of the kinetic data derived for the reactive angiotensin-type ions, the results are divided into two groups (1) ions that add three HI molecules during the reaction and (2) ions that add two HI molecules.

3.1. Addition of 3HI

The Ang-I $(M + H)^+$ ion provides three basic sites for the attachment of HI. If it is assumed that the ionizing proton is localized at the most basic site of the peptide (guanidinium group of arginine), then the reactive sites of the Ang-I $(M + H)^+$ ion are the N-terminus and the two histine side groups. Fig. 1 shows mass spectra generated by storing the singly charged Ang-I ion in HI (1.4×10^{-5} Torr, partial pressure in 1 mTorr of He) for different reaction times. The Ang-I $(M + H)^+$ ion follows three-step consecutive pseudo-first-order kinetics for:

$$(M + H)^+ \xrightarrow{k_1} (M + H + HI)^+ \xrightarrow{k_2} (M + H + 2HI)^+ \xrightarrow{k_3} (M + H + 3HI)^+ \quad (2)$$

To determine the reaction rates for each consecutive step of the reaction, many spectra, such as those shown in Fig. 1, were taken at various reaction times to generate the ion abundance profile for the reaction [Fig. 2(a)]. The value for the first rate (k_1) was determined by fitting the abundance of the $(M + H)^+$

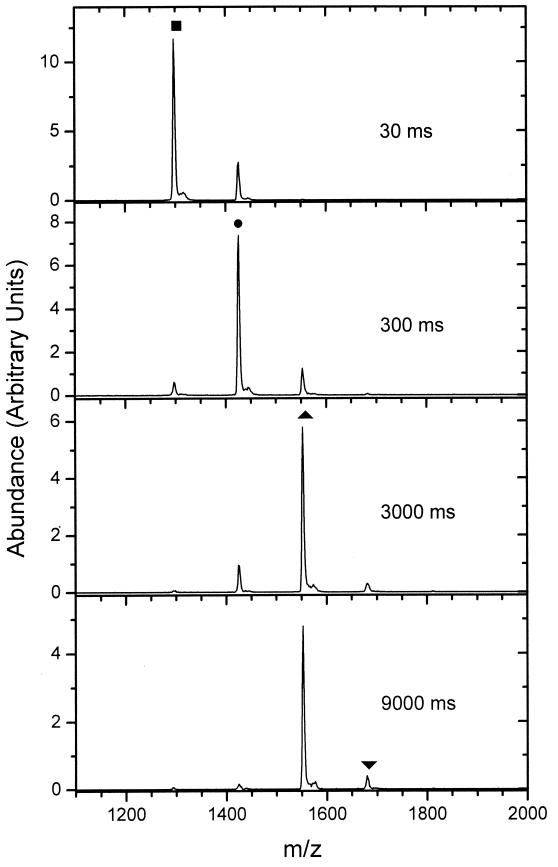

Fig. 1. Mass spectra obtained by storing Ang-I $(M + H)^+$ ions in the presence of 1.4×10^{-5} Torr HI for (a) 30, (b) 300, (c) 3000, and (d) 9000 ms. The symbols above peaks correspond to data points in Fig. 2.

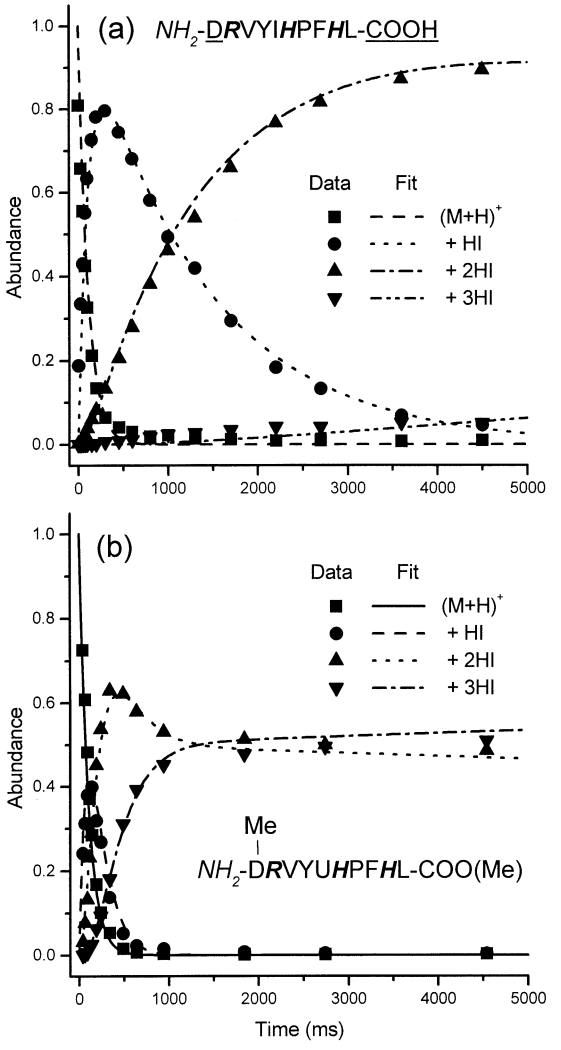

Fig. 2. Ion abundance profile for (a) Ang-I $(M + H)^+$ ions and (b) Ang-I methyl ester $(M + H)^+$ ions stored at 1.4×10^{-5} Torr HI and compiled from many spectra such as Fig. 1. The curves generated by fitting the experimental data to equations of the form shown in Eq. (1) are shown as broken lines (see legend).

ion to an exponential decay function [Eq. (1)]. The following consecutive steps were then fit simultaneously (with k_1 held constant). The rate constants shown in Table 1 were obtained by dividing the rates determined from the fits to the data by the number density of HI (e.g. 4.5×10^{11} cm^{-3} at 1.4×10^{-5} torr).

The modification (or removal) of one or both acidic groups of Ang-I has a direct effect on the rate constants for the addition of HI. In most cases, methylation lowers the rate constant for the addition of the first HI molecule (see Table 1). However, the subsequent additions of the second and third HI molecules were affected differently depending on the amino acid sequence of the ion. For Ang-I $(M + H)^+$ methyl ester, the first rate constant (k_1) for the multistep reaction shows no change, within experimental error, relative to the unmodified ion whereas both k_2 and k_3 show significant increases. The unmeasurable change in k_1 accompanied by a relatively large increase in k_2 and k_3 is indicative of a decrease in the reactivity for one attachment site, but an increase in reactivity for the other attachment sites. If this were not the case, a significant increase in k_1

Table 1
Angiotensin analogs—addition of 3HI

Peptide $(M + H)^+$	Sequence	k_1[a]	k_2[a]	k_3[a]
Ang-I	DRVYIHPFHL	3.5 ± 0.4	0.27 ± 0.05	0.007 ± 0.005
Ang-I-Me	DRVYIHPFHL-Me_2	3.7 ± 0.4	2.4 ± 0.3	0.55 ± 0.08
GF-Ang	NRVYVHPFHL	2.2 ± 0.2	1.4 ± 0.3	0.23 ± 0.06
GF-Ang-Me	NRVYVHPFHL-Me_1	1.4 ± 0.2	0.93 ± 0.14	0.23 ± 0.08
des-Asp[1] Ang-I	RVYIHPFHL	2.7 ± 0.3	1.3 ± 0.3	0.16 ± 0.07
des-Asp[1] Ang-I-Me	RVYIHPFHL-Me_1	0.71 ± 0.09	0.45 ± 0.08	0.45 ± 0.09

[a] Rate constants ($\times 10^{-11}$ cm^3 s^{-1}) as per Eq. (2).

would be expected based on the magnitudes of the increases in k_2 and k_3. However, only ~50% of the Ang-I-Me $(M + H)^+$ ions add the third HI at the increased reaction rate [Fig. 2(b)], thus indicating the presence of a second reactive population for the methylated Ang-I $(M + H)^+$ ions.

The substitution of asparginine for aspartic acid (GF-Ang-I) also creates the same general effect—lowering k_1, but raising k_2 and k_3 (Table 1). Likewise, removing the aspartic acid residue from the peptide (des Asp^1 Ang-I) lowers k_1 and raises k_2 and k_3. Thus, relative to the Ang-I $(M + H)^+$, modification of one or more acidic groups decreases the reactivity of one attachment site but increases the reactivity of the other attachment sites in the ion. The strong structural dependence on the carboxylic acid groups is also reflected in the reactivity of the doubly charged ions of Ang-I and its methyl ester, as well (see the following).

A very unusual reaction phenomenology, which has been observed thus far only for angiotensin-type ions, was the change in the ion reactivity upon addition of HI. For an ion/molecule reaction of the type shown in Eq. (2), the ratio k_1/k_2 should be greater than or equal to 2, or more generically:

$$k_m \geq \left(\frac{n}{m}\right) k_n, \quad n > m, \quad m = 1, 2, \ldots, n-1 \tag{3}$$

For linear first-order reaction kinetics, the rate constant of the first step in consecutive reactions is determined in part by the fastest reacting site. The presence of sites with equivalent reactivity sets the k_1/k_2 value at its minimum value of 2, and sites of lower reactivity cause k_1/k_2 to rise above 2. However, for most of the singly charged ions shown in Table 1 (Ang-I-Me and des-Asp^1-Ang-I, GF-Ang-I, and their respective O-methyl esters) the k_1/k_2 value is slightly lower than 2. The deviation from expected kinetic behavior can be seen graphically in Fig. 3, which shows the most extreme example—the des-Asp^1 Ang-I methyl ester $(M + H)^+$. Here, the decay of the $(M + H)^+$ ion and growth of the $(M + H + HI)^+$ follow the expected abundance profile. However, due to the higher k_2 value, the decay of the $(M + H + HI)^+$ and growth of the $(M + H + 2HI)^+$ ion begins at an earlier reaction time than expected, and likewise for the addition of the third HI. The disparity is most evident at reaction times >4000 ms, where the ion has reacted to completion [i.e. to $(M + H + 3HI)^+$], but under normal kinetic behavior [as per Eq. (3)] the intensities should show predominately the $(M + H + 2HI)^+$ ion at 4000 ms [arrows in Fig. 3(b)]. This unusual kinetic behavior is also seen for GF-Ang-II (see sec. 3.2.).

3.2. Addition of 2HI

The abundance profiles of Ang-I $(M + 2H)^{2+}$ and its respective methyl ester ion illustrate results from the presence of multiple ion populations (Fig. 4). For the Ang-I $(M + 2H)^{2+}$ ions, the majority of the ion population (~80%) reacts with 1 HI, but the remaining 20% is essentially unreactive on the time scale of our experiments [Fig. 4(a)]. A small amount of the reactive ion population (~5%) adds a second HI molecule at a very low rate, but the ion intensities change very little at reaction times longer than ~1000

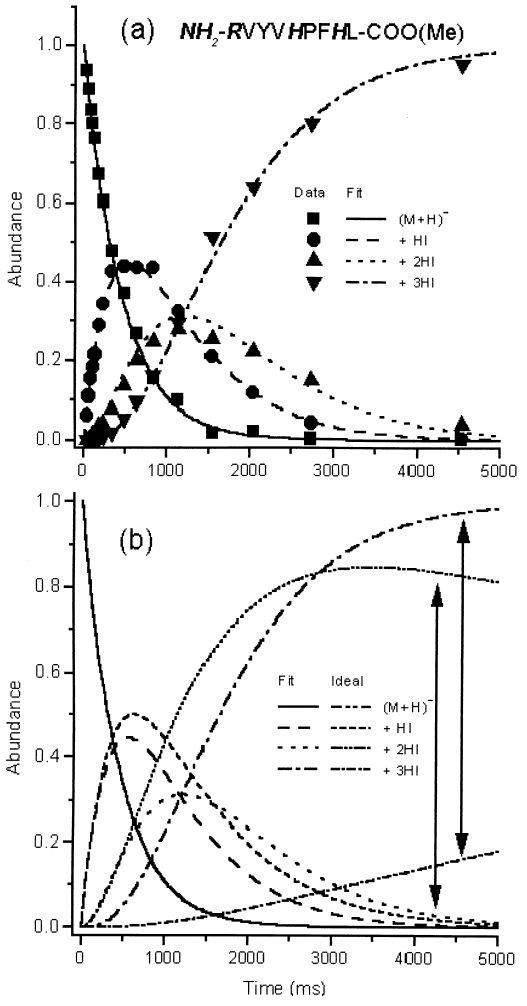

Fig. 3. Ion abundance profile for (a) des-Asp[1] methyl ester $(M + H)^+$ ions at 1.4×10^{-5} torr HI and the curves generated by fitting the data. (b) Comparison of the ideal ion abundance profile with the fits generated from the experimental results in (a).

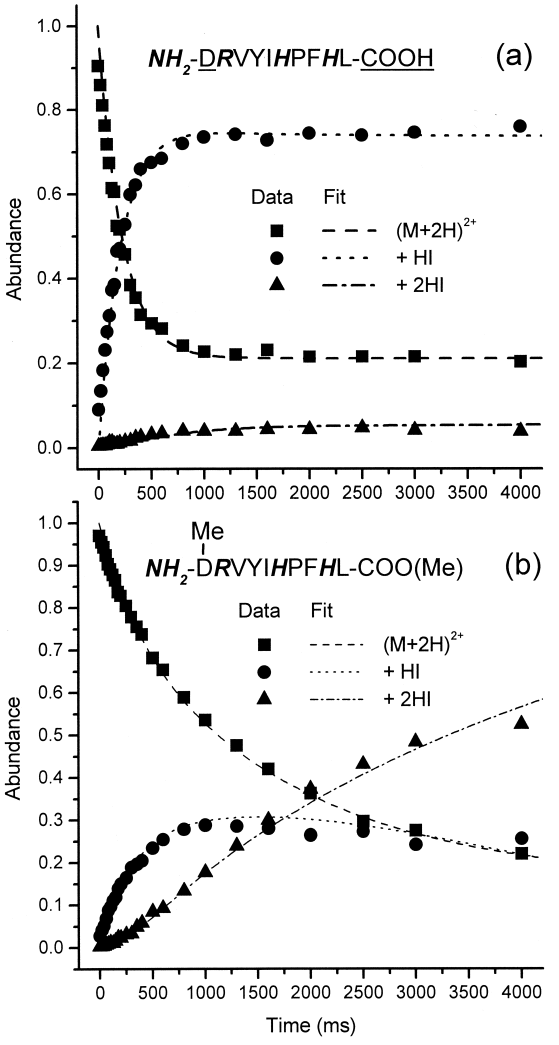

Fig. 4. As in Fig. 2, but for (a) Ang-I $(M + 2H)^{2+}$ and (b) Ang-I methyl ester $(M + 2H)^{2+}$.

ms. When methylated at the C-terminus and the Asp residue, the reactivity of the Ang-I $(M + 2H)^{2+}$ ion changes dramatically [Fig. 4(b)]. For Ang-I-Me $(M + 2H)^{2+}$, three ion populations are detected: the fast and slow reacting populations, and an unreactive population (20%). Like the singly charged $(M + H)^+$ ion, the abundance profile [Fig. 4(b)] and derived rate constants (Table 2) for the Ang-I-Me $(M + 2H)^+$ ion show that while methylation leads to no measurable change in the rate for the first addition of HI, it increases the rate of addition of the second HI molecule to the ion.

The addition of HI to $(M + 2H)^{2+}$ ions of GF-Ang-I (NRVYVHPFHL) and its methyl ester [Figs. 5(a) and 5(b), respectively] exhibit similar kinetics to those of the $(M + 2H)^{2+}$ ions of Ang-I and its methyl ester. The rate constants for the two reactive ion populations of GF-Ang-I $(M + 2H)^{2+}$ are slightly lower than the Ang-I $(M + 2H)^{2+}$ ion (Table 2). By methylating the C-terminus of this ion, the rate constant for the addition of the first HI is decreased

Table 2
Angiotensin analogs—addition of 2HI

Peptide		Fast				Slow		
$(M + nH)^{n+}$	Sequence	n	%[a]	k_1[b]	k_2[b]	%[a]	k_1[b]	k_2[b]
Ang-I	DRVYIHPFHL	+2	80	1.2 ± 0.2	0.0003 ± 0.0001	20	...	...
Ang-I-Me	DRVYIHPFHL-Me_2	+2	20	1.0 ± 0.2	0.49 ± 0.06	65	0.16 ± 0.02	0.08 ± 0.01
GF-Ang	NRVYVHPFHL	+2	40	0.78 ± 0.1	0.13 ± 0.03	40	0.11 ± 0.01	0.003 ± 0.001
GF-Ang-Me	NRVYVHPFHL-Me	+2	50	0.42 ± 0.03	0.21 ± 0.02	40	0.10 ± 0.03	0.002 ± 0.001
des-Asp^1 Ang-I	RVYIHPFHL	+2	100	0.021 ± 0.003	0.0005 ± 0.0001	...	...	...
des-Asp^1 Ang-I-Me	RVYIHPFHL-Me_1	+2	100	0.004 ± 0.001	...	...	...	...
Ang-II	DRVYIHPF	+1	70	5.1 ± 0.4	0.39 ± 0.05	30	2.3 ± 0.04	0.11 ± 0.03
Ang-II-Me	DRVYIHPF-Me_2	+1	70	2.5 ± 0.1	1.0 ± 0.2	30	2.5 ± 0.03	0.013 ± 0.02
GF-Ang-II	NRVYVHPF	+1	100	0.78 ± 0.09	0.75 ± 0.08	...	...	...
GF-Ang-II-Me	NRVYVHPF-Me_1	+1	100	2.5 ± 0.3	1.2 ± 0.2	...	...	...

[a] Ion populations determined by reaction kinetics.
[b] Rate constants ($\times 10^{-11}$ cm^3 s^{-1}).

for both reactive ion populations. In accordance with the kinetics of Ang-I and its methyl ester, the rate constant for the addition of the second HI increases for both reactive populations (fast and slow reacting) of GF-Ang-I-Me, relative to GF-Ang-I. However, unlike the Ang-I and its methyl ester $(M + 2H)^{2+}$ ions, the unreactive ion population decreases by 5% when the GF-Ang-I is methylated.

While the reactivity of the singly charged des-Asp^1 Ang-I (RVYIHPFHL) and its methyl ester ion was somewhat similar to that of the singly charged Ang-I, GF-Ang-I, and their methyl ester ions, the des-Asp^1 Ang-I $(M + 2H)^{2+}$ ion's reactivity is dramatically different from its doubly charged counterparts. The reaction kinetics for the des-Asp^1 Ang-I doubly charged ions are among the lowest for the angiotensin suite of ions. In fact, for the des-Asp^1 Ang-I methyl ester $(M + 2H)^{2+}$ the reaction rate for the addition of the first HI was barely above our measurement capabilities, and the rate of addition of the second HI to the ion could not be determined confidently (see Table 2).

The addition of the first HI to the smaller Ang-II $(M + H)^+$ ion proceeds with the highest rate constant among the ions studied here (5.1×10^{-11} cm^3 s^{-1}). The reaction kinetics for the addition of HI to this ion also indicates that two different reactive populations are present. The $(M + H)^+$ ion of the Ang-II methyl ester (methylated at Asp^1 and C-terminus) also shows two ion populations. However, these populations add the first HI at the same rate, but differ in the rate of addition for the second HI molecule. Thus, like the Ang-I ions methylation causes both a decrease in the rate of addition for the first HI and an increase the rate of addition of the second HI.

The $(M + H)^+$ ion of GF-Ang-II shows reaction kinetics that are similar to those seen in the singly charged des-Asp^1 Ang-I methyl ester ion. The rate constants for GF-Ang-II $(M + H)^+$ also show a substantial deviation from the ideal ($k_1/k_2 = 2$) kinetic behavior [see Fig. 6(a) and Table 2] expected for this type of ion molecule reaction. In contrast with this unusual kinetic behavior, the GF-Ang-II methyl ester $(M + H)^+$ shows ideal pseudo-first-order reaction kinetics [Fig. 6(b)]. Not only does this ion show a single reacting population, the k_1/k_2 ratio of 2 (see Table 2) is consistent with two equivalent reactive sites in the ion.

4. Calculations and discussion

The rate constants for the angiotensin/HI reactions were found to be of the same order of magnitude as the bradykinin/HI reactions [42]. However, no rate constant was observed to be as great as that of the fastest addition of HI to the bradykinin $(M + H)^+$ ion, which presumably reacts through the guanidinium group of one of the arginine residues. Since

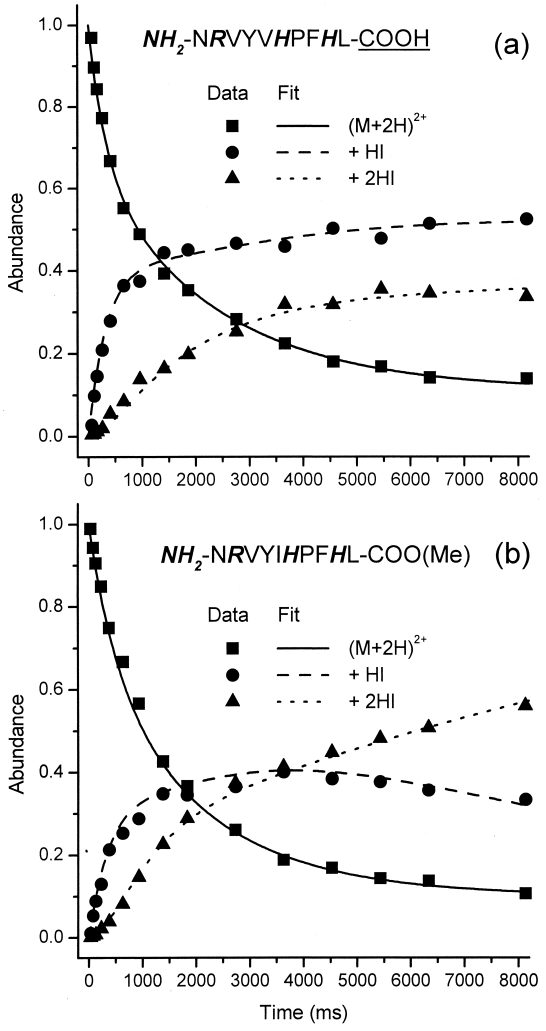

Fig. 5. As in Fig. 2, but for (a) GF-Ang-I $(M + 2H)^{2+}$ and (b) GF-Ang-I methyl ester $(M + 2H)^{2+}$.

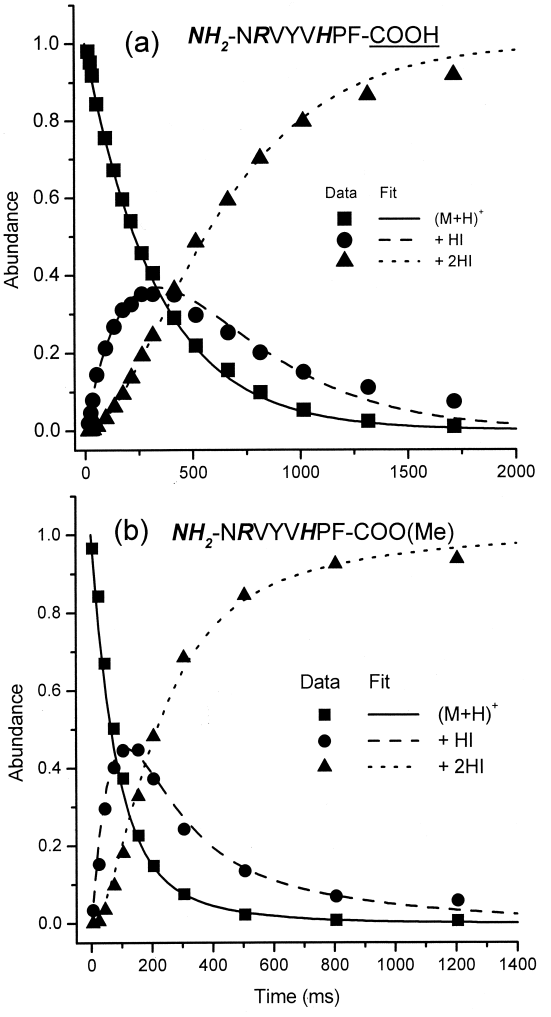

Fig. 6. As in Fig. 2, but for (a) NRVYVHPF $(M + H)^{+}$ and (b) the $(M + H)^{+}$ ion of the methyl ester.

only one arginine residue is present in the angiotensin suite of ions, protonation at the guanidinuim group can be expected based on previous arguments concerning gas phase basicity (GB) of this functional group [52–54]. Thus, the reactive sites remaining for the addition of HI should be the N-terminus and histidine side groups. Through previous studies, it was suggested that the rate constant attachment of HI to protonated peptides generated by electrospray ionization is dependent on two factors: (1) the magnitude of [GB (reactive site) $-\ \Delta G_{acid}$(HI)] and (2) the exposure of the reactive site in the peptide ion. For the singly charged angiotensin ions studied here, if it is assumed that protonation occurs at the guanidinium group of the arginine residue, all ion/molecule reactions should show nearly equivalent reactivities (on a per-site basis) because the reactive sites should be either histidine or the amino-terminus. However, this is clearly not the case. Thus, steric factors may play an integral role in determining the HI addition kinetics for this class of ions.

To gain insight into the steric factors and intra-ionic interactions that influence the reaction kinetics,

molecular mechanics calculations were performed to evaluate ion structures that provide a rationale for the observed kinetics. The molecular mechanics calculations suggest a substantial degree of intraionic hydrogen bonding in this family of angiotensin-related ions, which is similar to that reported for other polypeptide ions in the gas phase [13,29,37]. For the singly protonated peptides, a prevalent structural motif seems to dominate for this suite of ions when the protonation site is the guanidinium group of arginine. The localized charge is typically solvated in the interior of the ion by hydrogen-bonding between the protonated guanidinium group and other basic sites in the ions (e.g. amide carbonyls, histidine, N-terminus). In fact, many of the candidate structures (~1/2) obtained for the angiotensin analogs exhibited hydrogen bonds between this charge group and one (or both) of the histidine residues, which are potential reactive sites for the addition of HI. For example, the minimized structure of GF-Ang-I exhibited H bonding between the guanidinium charge site and the Pro^7 carbonyl and the His^9 histine group, but the other two reactive groups (N-terminus and His^6) were fully exposed to HI attack (i.e. not H bonded to the charge site and not buried in the interior of the ion).

Relative to other $(M + H)^+$ ions with similar amino acid sequences and reactive sites, the kinetics for HI attachment to Ang-I $(M + H)^+$ are much slower for the addition of the second and third HI molecule to the ion. Since the identities of the reactive sites in question are presumably the same for the $(M + H)^+$ ions of Ang-I, GF-Ang-I, des-Asp^1-Ang-I and their methyl esters, the difference in reaction kinetics is likely conformational in origin. Fig. 7 shows the geometry minimized structures of Ang-I $(M + H)^+$ [Fig. 7(a)] and its methyl ester [Fig. 7(b)]. The Ang-I $(M + H)^+$ ion was the *only* ion studied that showed extensive H bonding with both reactive histine groups. The minimized geometry of the Ang-I methyl ester $(M + H)^+$ ion also showed H bonding between the protonated guanidinium group and surrounding basic sites, but showed H bonding only to the His^6 histine group, and is quite representative of the structures that are obtained for many of the other analogs of Ang-I. These structural models are qualitatively consistent with the observed reaction kinetics for these two ions.

Comparing the reaction kinetics for the methylated and nonmethylated Ang-I ions also indicated the critical role that the acidic groups play in the reaction kinetics, which was also observed for bradykinin ions [42]. As can be seen in the rate constants for both the singly and doubly charged ions of methylated and nonmethylated Ang-I, blocking of the acidic groups by a methyl group increases the rate of addition for the second and third HI molecules to the ion. The disruption of the intraionic interactions found in the non-methylated ions involving the acidic groups [see, e.g. the position of the carboxylic acid groups in Fig. 7(a) and (b), respectively] are predicted to affect significantly the structure of the ion. As can be seen in the structure of the Ang-I methyl ester [Fig. 7(b)], the methyl ester groups are now in dramatically different positions and one of the reactive sites has repositioned to the exterior of the ion and is no longer hydrogen bonded to the guanidinium charge site. Likewise, removal (des-Asp^1) or modification (goosefish) of a single carboxylic acid group in the peptide has the same general effect on the reaction rate constants and produced quite similar structures in the molecular mechanics simulations.

Since the geometry minimized structure is only loosely related to that of the reactive structure at room temperature, the structure of Ang-I $(M + H)^+$ that is shown in Fig. 7 was raised to 300 K and its structure parameters followed for 16.5 ns (Fig. 8). From the interatomic distances between the histine nitrogens of His^6 [Fig. 8(a)] and His^9 [Fig. 8(b)] and each of the hydrogens of the protonated guanidinium group, it is evident that the two histidine groups are hydrogen bonded to at least one of the charge-site hydrogens for the duration of the simulation. Similarly, this illustrates that the local structure around the charge-carrying moiety does not change appreciably over the simulation duration. Thus, the type of intraionic bonding in this particular ion, which is predicted by the molecular mechanics simulation, illustrates how a reactive site in a peptide may be blocked from attack by an HI molecule if the reactive site is involved in solvating the ion charge.

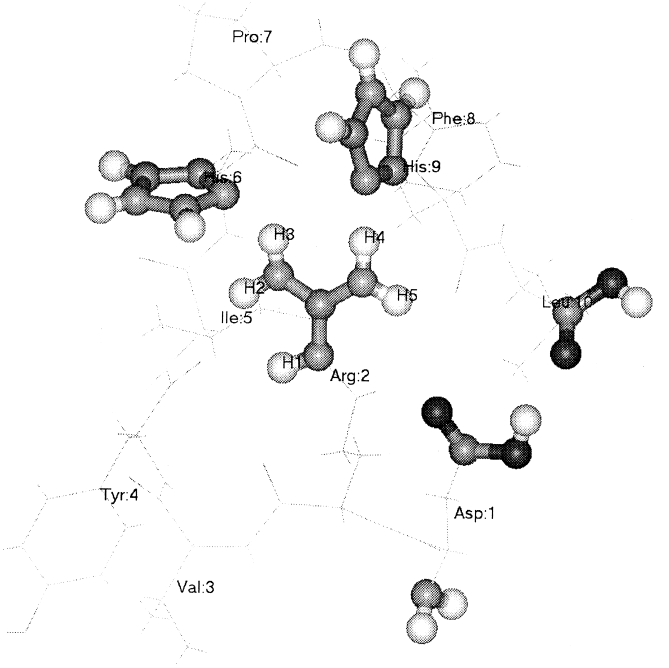

(a)

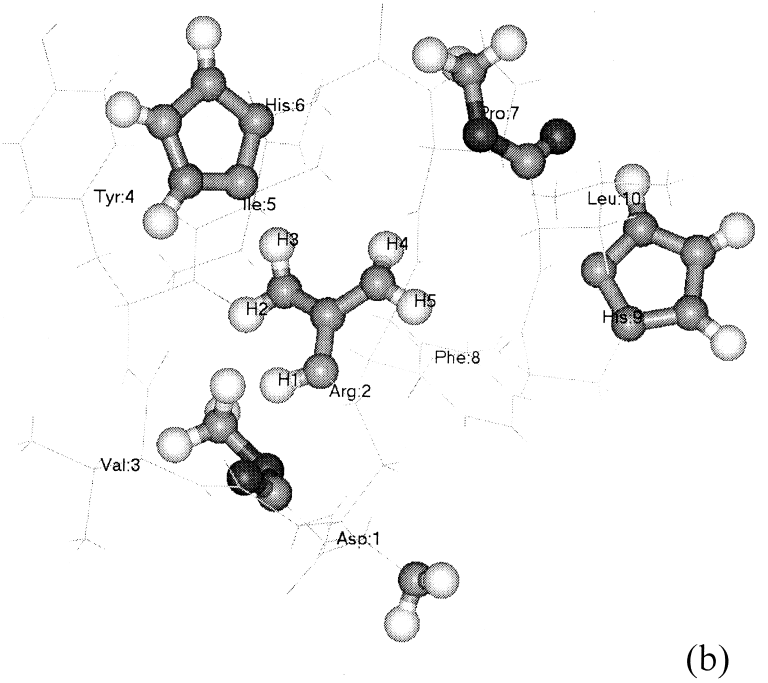

(b)

Fig. 7. Geometry minimized structure obtained for the $(M + H)^+$ ions of (a) Ang-I and (b) Ang-I methyl ester. The (reactive) basic and carboxylic acid sites are shown as ball and stick, and the rest of the structure as lines. Note the close proximity of the His^6 and His^9 groups to the guanidinium charge site. The atomic labels (H1–H5, N6, and N9) on Ang-I $(M + H)^+$ (a) correspond to the labels shown in Fig. 8.

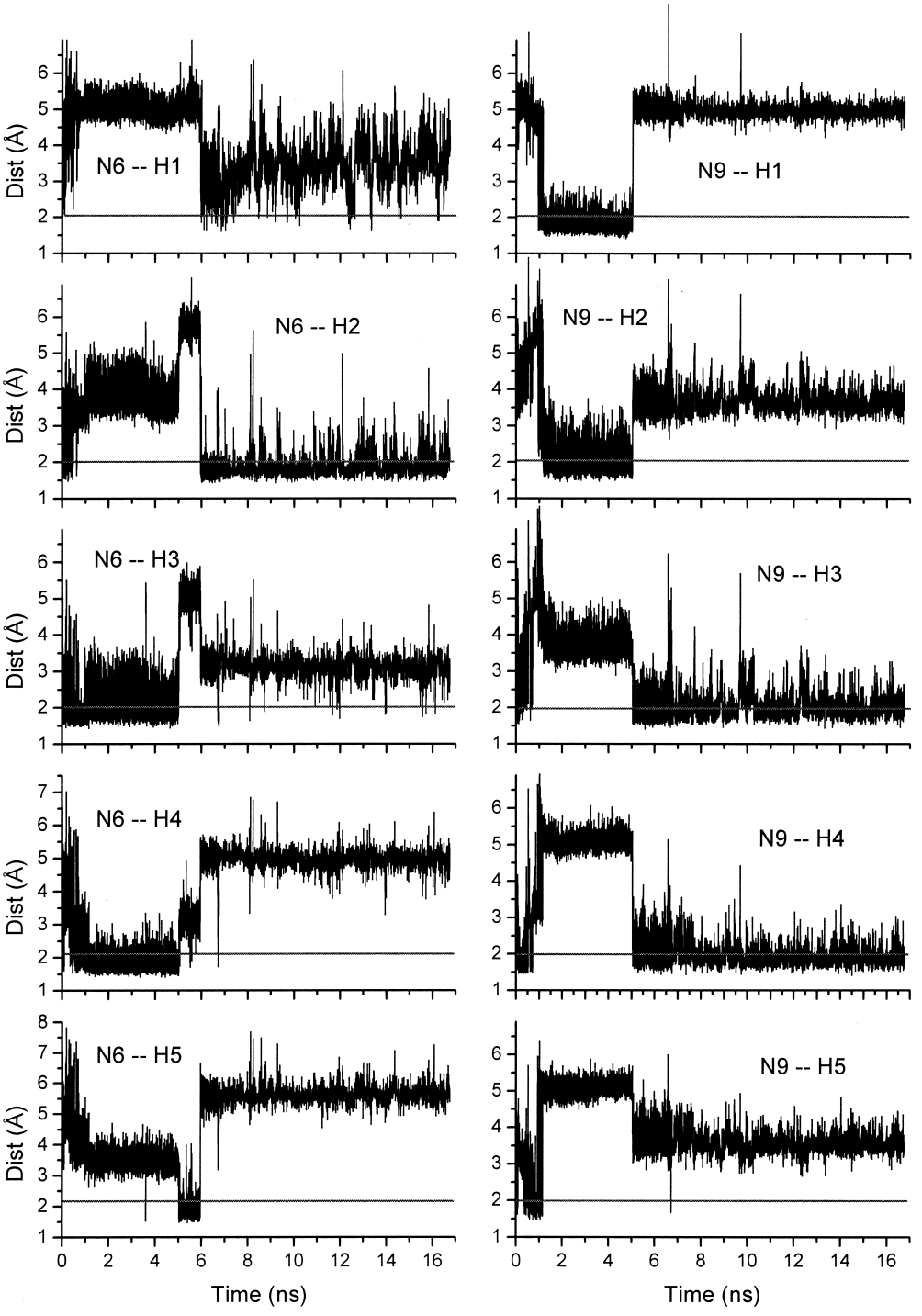

Fig. 8. Hydrogen bond distances between the histine (N6, N9) groups of His[6] (left-hand column) and His[9] (right-hand column) and each of the hydrogens (see labels) of the protonated guanidinium group at 300 K for 16.7 ns. The notation used for each of the graphs corresponds to the atom labels shown in Fig. 7.

The experimental data reported here cannot preclude the possible role of salt bridges in the polypeptides comprised of both acidic and basic functionalities. Strong evidence for such interactions in bradykinin ions has already been presented [37]. Furthermore, in our previous work with the attachment of HI to bradykinin ions we alluded to the possibility that such interactions might explain the reduction in attachment rates associated with methyl esterification of bradykinin ions and its analogs. It was reasoned that the addition of a molecule of HI could stabilize an intramolecular acid–base interaction by insertion and thereby enhance the rate of HI attachment relative to the methyl esterified ion. However, the molecular mechanics calculations described here indicate that intramolecular acid–base interactions between carboxy groups and one or more of the histidine residues need not be invoked to rationalize the kinetic data reported here. Rather, the interactions between the histidines and the quanidinium moiety are apparently the dominant phenomena in determining relative HI attachment kinetics.

The extensive intraionic interactions suggested by the molecular mechanics simulations also provide a rationale for the deviation from ideal pseudofirst order kinetics where the reactivity increases after HI addition. In order for this type of kinetic behavior to occur, the reactivity of the ion must change during the addition of the first or second HI molecule. Thus, it is evident that the attachment of HI to the ions can induce a change in the ion structure, and hence a change in the ion reactivity. Any disruption of the intra-ionic hydrogen bonding by the insertion of HI into the ion structure can conceivably expose reactive sites that were previously blocked in the native (as obtained from electrospray ionization) gas phase structure. For Ang-I-Me, des-Asp^1 Ang-I, GF-Ang-I, and GF-Ang-I-Me, the deviation from the expected maximum for k_1/k_2 is small and nonexistent for k_2/k_3 [i.e. $k_2 > 3/2(k_3)$]. However, for des-Asp^1-Me and GF-Ang-II the deviation is quite large. Thus, for these two ions, we can assume that the perturbation of the ion structure upon attachment of HI is relatively large compared to the other singly charged ions shown in Tables 1 and 2. It should be noted, though, that the ions of angiotensin and all of its analogs (to include the O-methyl ester derivatives) are the only set of ions studied thus far (out of 40+ peptides and proteins) that exhibit this reaction effect.

The molecular mechanics simulations of the doubly charged ions are not as straightforward to interpret as the singly charged ions due to the uncertainty involved in the location of the ionizing protons, and thus, the detailed analysis of these calculations is beyond the scope of this report. However, for the doubly charged ion of Ang-I, structures with similar total energies (within a ±5% window) can be generated having a variety of geometries. For instance, the total energy of Ang-I $(M + 2H)^{2+}$ geometry minimized structures generated by protonating the N-terminus and guanidinium group falls within a 0–5% window of the Ang-I $(M + 2H)^{2+}$ ion generated by protonating the His^9 and guanidinium group. However, protonation of the His^6 and guanidinium group generates structures having total energies a full 15%–20% higher than the other two possibilities. Thus, the presence of multiple ion conformations for the doubly charged ions of this class of ions may simply lie in the identities of the protonation sites and the identities and relative exposures of the remaining reactive sites. For instance, the two reactive populations seen with Ang-I $(M + 2H)^{2+}$ may arise from conformations in which the second ionizing proton is associated with either the N-terminus or the His^9 position, but likely not at the His^6 position.

The presence of multiple ion conformations has been alluded to in many reports involving both ion/molecule reactions and ion mobility cross-sectional measurements. However, here we concentrate primarily on the report of Freitas and co-workers because of the ions investigated in their study [38]. Specifically, the H/D exchange of angiotensin-I, -II, and -III ions were examined. It is interesting to note that both H/D exchange kinetics and HI addition kinetics reveal at least two gas phase reactive populations for the Ang-II $(M + H)^+$ ions, but only one reactive population for the Ang-I $(M + H)^+$ ions. Thus, comparing these two studies, HI attachment kinetics provides both complementary information concerning the availability of reactive sites for HI

attachment and supporting information for the presence of multiple reactive ion populations.

Since the first HI addition reactions with polypeptides were performed, we have searched for a gas phase polypeptide ionic system that exhibits equilibrium kinetics. The ion/molecule reaction profile seen in Fig. 5 presents the best possibility, thus far, for finding such a system. To probe the possibility of this system reaching equilibrium, the ions (as generated from electrospray) were allowed to react for ~2000 ms, where the ion intensities become static. Then both the reactant and product ions were *re*-selected and stored again, in turn. No further reaction was measured for the re-isolated $(M + 2H)^{2+}$ ion population (~20% of original ion population). Likewise, when the HI addition product ions were isolated and stored, the reverse reaction was not observed for either the $(M + 2H + HI)^{2+}$ or the $(M + 2H + 2HI)^{2+}$ ions. Thus, the essentially static ion abundances observed at times greater than about 2000 ms must be interpreted as reflecting inherent reactivity differences in a multicomponent ion population (i.e. different ion conformations) and not simply an approach to equilibrium conditions.

5. Conclusions

The kinetics for the gas phase addition of HI to the ions of angiotensin-I, angiotensin-II, and their structural analogs were presented. The gas phase reaction kinetics show that HI can be used to detect the presence of multiple ion conformations and monitor changes in the ion structure, as it relates to the reactivity of the ions. In some cases though, the addition of HI can induce structural changes in the ion, as revealed through the reaction kinetics. These changes may cause subtle or dramatic deviations from the expected ion/molecule reaction kinetics. For bradykinin ions, and many other ions studied thus far, the HI addition kinetics can be explained generally as being governed by the gas phase basicity of the reactive site and its exposure to attack by HI. However, for more complicated polypeptides (i.e. containing multiple acidic and basic residues), in which strong intraionic interactions play an important role in determining the three-dimensional structure of the ion, the addition of HI can alter the interactions giving rise to changes in structure/reactivity that depends upon the number of attached molecules of HI.

The kinetic behavior of the singly charged Ang-I and its analogs is consistent with the molecular mechanics calculations. The blocking of potential reactive sites through charge solvation and the strong intra-ionic interactions suggested by the molecular mechanics simulations fit well with all aspects of the special reactive nature of the angiotensin ions: (1) the slow reaction kinetics for the addition of multiple HI molecules, (2) the change in ion reactivity upon addition of HI, and (3) the dramatic change in reactivity upon methylation of carboxylic acid groups.

The evidence shown here for structural changes occurring upon addition of a molecule of HI to a polypeptide ion indicate that care must be taken in the use of HI attachment as a structural probe. Conversely, structural changes induced by the attachment of HI might be regarded as a kind of *gas-phase denaturing reaction*, in which HI can disrupt potentially detrimental intra-ionic bonding that causes inefficient fragmentation or other unwanted gas phase properties in polypeptides.

Acknowledgements

This research was sponsored by the National Institutes of Health under grant no. GM45372. Oak Ridge National Laboratory is managed by Lockheed Martin Energy Research Corporation for the U.S. Department of Energy under contract no. DC-AC05-96OR22464. The authors acknowledge Dr. Paul D. Schnier and Dr. William D. Price for many helpful discussions concerning the molecular modeling. One of the authors (T.G.S.) acknowledges support through appointments to the Oak Ridge National Laboratory Postdoctoral Research Associates Program administered jointly by the Oak Ridge Institute for Science and Education and Oak Ridge National Laboratory.

References

[1] G. Siuzdak, Proc. Natl. Acad. Sci. USA 91 (1994) 11290.
[2] J.R. Yates, Methods Enzymol. 271 (1996) 351.
[3] D.F. Hunt, N.-Z. Zhu, J. Shabanowitz, Rapid Commun. Mass Spectrom. 3 (1989) 122.
[4] J.A. Loo, C.G. Edmonds, R.D. Smith, Science 248 (1990) 201.
[5] R.D. Smith, C.J. Barinaga, H.R. Udseth, J. Chem. Phys. 93 (1989) 5019.
[6] A.L. McCormack, J.L. Jones, V.H. Wysocki, J. Am. Soc. Mass Spectrom. 3 (1992) 859.
[7] A.L. McCormack, A. Somogyi, A.R. Dongre, V.H. Wysocki, Anal. Chem. 65 (1993) 2859.
[8] J. Qin, B.T. Chait, J. Am. Chem. Soc. 117 (1995) 5411.
[9] S. Campbell, M.T. Rodgers, E.M. Marzluff, J.L. Beauchamp, J. Am. Chem. Soc. 117 (1995) 12840.
[10] A.R. Dongre, J.L. Jones, A. Somogyi, V.H. Wysocki, J. Am. Chem. Soc. 117 (1996).
[11] C.G. Gu, A. Somogyi, V.H. Wysocki, K.F. Medzihradszky, Anal. Chim. Acta 397 (1999) 247.
[12] G. Tsaprailis, H. Nair, A. Somogyi, V.H. Zhong, J.H. Futrell, S.G. Summerfield, S.J. Gaskell, J. Am. Chem. Soc. 121 (1999) 5142.
[13] S.G. Summerfield, A. Whiting, S.J. Gaskell, Int. J. Mass Spectrom. Ion Processes 162 (1997) 149.
[14] R.E. Gimon-Kinsel, D.C. Barbacci, D.H. Russell, J. Mass Spectrom. 34 (1999) 124.
[15] K.A. Cox, S.J. Gaskell, M. Morris, A. Whiting, J. Am. Soc. Mass Spectrom. 7 (1996) 522.
[16] G.A. Eiceman, Crit. Rev. Anal. Chem. 22 (1991) 17.
[17] M.F. Jarrold, J.E. Bower, J. Phys. Chem. 97 (1993) 1746.
[18] G. von Helden, M.T. Hsu, N. Gotts, M.T. Bowers, J. Phys. Chem. 97 (1993) 8182.
[19] S.J. Valentine, A.E. Counterman, D.E. Clemmer, J. Am. Soc. Mass Spectrom. 8 (1998).
[20] J. Woenkhaus, Y. Mao, M.F. Jarrold, J. Phys. Chem. B 101 (1997) 847.
[21] M.K. Green, C.B. Lebrilla, Mass Spectrom. Rev. 16 (1997) 53.
[22] K.B. Shelimov, M.F. Jarrold, J. Am. Chem. Soc. 119 (1997) 2987.
[23] J. Woenckhaus, R.R. Hudgins, M.F. Jarrold, J. Am. Chem. Soc. 119 (1997) 9586.
[24] M.F. Jarrold, Acc. Chem. Res. 32 (1999) 360.
[25] A.E. Counterman, S.J. Valentine, C.A. Srebalus, S.C. Henderson, C.S. Hoaglund, D.E. Clemmer, J. Am. Soc. Mass Spectrom. 9 (1998) 743.
[26] K.B. Shelimov, D.E. Clemmer, R.R. Hudgins, M.F. Jarrold, J. Am. Chem. Soc. 119 (1997) 2240.
[27] S.J. Valentine, A.E. Counterman, D.E. Clemmer, J. Am. Soc. Mass Spectrom. 8 (1997) 954.
[28] E. Gard, M.K. Green, J. Bregar, C.B. Lebrilla, J. Am. Soc. Mass Spectrom. 5 (1994) 623.
[29] T. Wyttenbach, M.T. Bowers, J. Am. Soc. Mass Spectrom. 10 (1999) 9.
[30] S.A. McLuckey, G.J. VanBerkel, G.L. Glish, J. Am. Chem. Soc. 112 (1990) 5668.
[31] B.E. Winger, K.J. Light-Wahl, R.D. Smith, J. Am. Soc. Mass Spectrom. 3 (1992) 624.
[32] M.G. Ikonomou, P. Kabarle, Int. J. Mass Spectrom. Ion Processes 117 (1992) 283.
[33] D. Suckau, Y. Shi, S. Beu, M.W. Senko, J.P. Quinn, F.M. Wampler, F.W. McLafferty, Proc. Natl. Acad. Sci. USA 90 (1993) 790.
[34] P.D. Schnier, D.S. Gross, E.R. Williams, J. Am. Chem. Soc. 117 (1995) 6747.
[35] D.S. Gross, S.E. Rodriguez-Cruz, E.R. Williams, J. Phys. Chem. 99 (1995) 4034.
[36] C.J. Cassady, S.R. Carr, J. Mass Spectrom. 31 (1996) 247.
[37] P.D. Schnier, W.D. Price, R.A. Jockusch, E.R. Williams, J. Am. Chem. Soc. 118 (1996) 7178.
[38] M.A. Freitas, C.L. Hendrickson, M.R. Emmett, A.G. Marshall, J. Am. Soc. Mass Spectrom. 9 (1998) 1012.
[39] M.A. Freitas, A.G. Marshall, Int. J. Mass Spectrom. 183 (1999) 221.
[40] J.L. Stephenson, S.A. McLuckey, Anal. Chem. 69 (1997) 281.
[41] J.L. Stephenson, S.A. McLuckey, J. Am. Chem. Soc. 119 (1997) 1688.
[42] T.G. Schaaff, J.L. Stephenson, S.A. McLuckey, J. Am. Chem. Soc. 121 (1999) 8907.
[43] J.L. Stephenson, T.G. Schaaff, S.A. McLuckey, J. Am. Soc. Mass Spectrom. 10 (1999) 552.
[44] T.G. Schaaff, J.L. Stephenson, S.A. McLuckey, J. Am. Soc. Mass Spectrom. 11 (2000) 167.
[45] A.L. Lehninger, D.L. Nelson, M.M. Cox, Principles of Biochemistry, Worth, New York, 1993.
[46] G.C. Thorne, K.D. Ballard, S.J. Gaskell, J. Am. Soc. Mass Spectrom. 1 (1990) 249.
[47] G.J. vanBerkel, G.L. Glish, S.A. McLuckey, Anal. Chem. 62 (1990) 1284.
[48] J.E. Bartmess, R.M. Georgiadis, Vacuum 33 (1983) 149.
[49] G. vonHelden, T. Wyttenbach, M.T. Bowers, Int. J. Mass Spectrom. Ion Processes 146/147 (1995) 349.
[50] S. Lee, T. Wyttenbach, M.T. Bowers, Int. J. Mass Spectrom. Ion Processes 167 (1997) 605.
[51] J.W. Haefner, Modeling Biological Systems: Principals and Applications, Chapman and Hall, New York, 1996.
[52] G.S. Gorman, I.J. Amster, J. Am. Chem. Soc. 115 (1993) 5729.
[53] I.A. Kaltashov, D. Fabris, C.C. Fenselau, J. Phys. Chem. 99 (1995) 10046.
[54] I.A. Kaltashov, C.C. Fenselau, J. Am. Chem. Soc. 117 (1995) 9906.